NAD+-SIRT1 control of H3K4 trimethylation through circadian deacetylation of MLL1

Lorena Aguilar-Arnal, **Sayako Katada**[2], **Ricardo Orozco-Solis**, and **Paolo Sassone-Corsi**

Center for Epigenetics and Metabolism, U904 INSERM, Department of Biological Chemistry, School of Medicine, University of California Irvine, CA, USA

Abstract

The circadian clock controls the transcription of hundred genes through specific chromatin remodeling events. The histone methyltransferase Mixed-Lineage Leukemia 1 (MLL1) coordinates recruitment of CLOCK–BMAL1 activator complexes to chromatin, an event associated to cyclic H3K4 tri-methylation at circadian promoters. Remarkably, in mouse liver circadian H3K4me3 is modulated by SIRT1, a NAD^+ dependent deacetylase involved in clock control. We show that mammalian MLL1 is acetylated at two conserved residues, K1130 and K1133. Notably, MLL1 acetylation is cyclic, controlled by the clock and by SIRT1, and impacts the methyltransferase activity of MLL1. Moreover, H3K4 methylation at clock-controlled gene promoters is influenced by pharmacological or genetic inactivation of SIRT1. Finally, MLL1 acetylation and H3K4me3 levels at circadian gene promoters depend on NAD^+ circadian levels. These findings reveal a previously unappreciated regulatory pathway between energy metabolism and histone methylation.

Introduction

A wide variety of biological processes are under circadian control, as illustrated by rhythms in mammalian behavior, physiology and metabolism[1]. The core transcription factors CLOCK–BMAL1 dimerize to drive the expression of clock controlled genes (CCGs), a mechanism that relies on coordinated chromatin remodeling events[2]. Circadian transcription is associated to rhythmic changes on epigenetic marks at circadian promoters, such as H3K4 trimethylation (H3K4me3) and H3K9 and K14 acetylation [3,4]. A key event in circadian transcriptional activation is the CLOCK–BMAL1 interaction with the COMPASS complex component MLL1, whose enzymatic activity leads to the transcriptional activating histone mark, H3K4me3 (Ref. 5). MLL1 contributes to the recruitment of CLOCK–BMAL1 to chromatin and thereby to promoters of CCGs[5].

Cellular metabolism and the epigenome intersect at various levels [1,6] and the circadian clock has been proposed to control part of this interplay at least through the NAD$^+$-dependent deacetylase class of sirtuins[7]. In addition, the intracellular levels of many metabolites oscillate in a circadian manner[8,9]. Specifically, coenzyme NAD$^+$ levels fluctuate in a circadian manner thereby inducing rhythmicity in SIRT1 enzymatic activity[10–12]. Remarkably, NAD$^+$ oscillation is dictated by CLOCK–BMAL1 which directly control the gene *Nampt*, encoding the nicotinamide phosphoribosyltransferase (NAMPT) enzyme, the rate limiting step in the NAD$^+$ salvage pathway[11,12]. Moreover, genetic ablation or pharmacological inhibition of SIRT1 activity alters circadian rhythmicity of CCGs [10,13–15]. Also, as previously reported, SIRT1 appears to control circadian H3K9 and K14 acetylation at a number of CCGs promoters and regulate the expression of a specific, large subset of circadian genes[10,15,16].

While these studies have shown that circadian regulators operate in response to diverse cellular metabolic cues, the molecular mechanisms governing their crosstalk remain largely unexplored. One of the unanswered questions is indeed related to whether cyclic chromatin modifications are causally linked by control exerted by the circadian clock. Hence, we sought to determine whether the H3K4 methyltransferase MLL1 function on circadian gene promoters is influenced by metabolic regulation governed by the circadian clock. Here, we present evidence that the function of the metabolite NAD$^+$ extends to modulation of the circadian epigenome through a molecular interplay between SIRT1 and MLL1. As a consequence, levels on the epigenetic mark H3K4me3 at circadian gene promoters are responsive to intracellular NAD$^+$. We found that MLL1 is an acetyl-protein and that its enzymatic activity is controlled by SIRT1-dependent deacetylation. These findings may provide new insights into the circadian alterations that occur during aging, in which NAD$^+$ decay is paralleled by miss-regulation in amplitude and phase of clock controlled genes[14,17–19].

Results

SIRT1 controls cyclic levels of H3K4 trimethylation

During our studies on the role of SIRT1 in circadian transcription, we performed chromatin immunoprecipitation (ChIP) assays at different circadian times in dexamethasone synchronized wild type (WT) and SIRT1-deficient (*Sirt1*$^{-/-}$) mouse embryonic fibroblasts (MEFs). As previously reported, H3K4me3 displays robust circadian oscillation on *Dbp* promoter and coding region, being high at circadian time (CT) 18 and low at CT 30 (Refs. 4,5) (Fig. 1a, *Dbp* E1 and *Dbp* I1). Analogous results were obtained in several CCGs, including *Per2*. Also, H3K4me3 levels in *Sirt1*$^{-/-}$ MEFs, exhibit markedly higher levels than in WT MEFs along the circadian cycle (Fig. 1a, *Dbp* E1 and *Dbp* I1), an intriguing observation since H3K4me3 and H3K9 and K14 acetylation have been functionally associated[20].

To explore whether the increase of H3K4me3 is directly linked to SIRT1, we treated WT MEFs with the specific inhibitor EX527. This treatment results in increase of H3K4me3 at *Dbp* coding region (Fig. 1a, *Dbp* E1 and *Dbp* I1), but not on the 3′ untranslated region (UTR) used as control for specificity (Fig. 1a). Analogous results were obtained *in vivo* by

analyzing livers from mice *Sirt1 Ex4*, which present a liver-specific deletion in the catalytic domain of the *Sirt1* gene [10,21]. Indeed, similarly to MEFs, H3K4me3 levels at circadian gene promoters show higher amplitudes when *Sirt1* is mutated as compared to wild type littermates (Fig. 1b), a difference associated to parallel changes in circadian gene expression (Supplementary Fig. 1a,b). Importantly, H3K4me3 and expression levels from the non-circadian housekeeping genes *Tbp* and *Gapdh*, and the MLL1-controlled genes *HoxA9* and *Emilin1* (Refs. 22–24) display no significant changes upon *Sirt1* deletion (Fig. 1c and Supplementary Fig. 1c,d). Thus, SIRT1 appears to control specifically a subset of MLL1 targets, namely circadian genes. These results highlight the specificity of the control of the circadian epigenome at clock-controlled genes, which are governed by a dedicated molecular machinery to maintain the correct circadian output. Also, H3K4me1 levels do not cycle, neither are altered upon deletion or pharmacological inhibition of SIRT1 (Supplementary Fig. 2a). On the other hand, H3K4me2 levels at the *Dbp* gene are increased in *Sirt1*$^{-/-}$ MEFs, and when cells are treated with EX527 (Supplementary Fig. 2a). Thus, SIRT1 appears to specifically affect H3K4 circadian methylation levels at CCGs.

NAD$^+$-dependent cyclic H3K4 trimethylation

NAD$^+$ metabolism is intimately linked to circadian rhythms. The NAD$^+$ salvage pathway is clock-controlled since the expression of the rate-limiting enzyme NAMPT is driven by the clock[11,12]. NAD$^+$ levels are circadian, leading to cyclic SIRT1 enzymatic activity[10,11]. Since our findings suggest a crosstalk between energy metabolism and the epigenetic modifier MLL1, we explored whether alterations in the levels of intracellular NAD$^+$ would influence MLL1-mediated circadian gene transcription (Fig. 1d). Increasing doses of NAD$^+$ progressively dampened MLL1-mediated activation of *Dbp* and *Per1* expression (Fig. 1d and Supplementary Fig. 2b). Also, the NAD$^+$ precursorsβ–nicotinamide mononucleotide (β–NMN) and nicotinic acid (NA) elicited a similar effect (Fig. 1d and Supplementary Fig. 2b). The treatment with the by-product of NAD$^+$ consumption, NAM, elicited a substantial and dose-dependent increase in MLL1-mediated activation of *Dbp* expression (Fig. 1d and Supplementary Fig. 2b). A similar trend was apparent in *Sirt1*$^{-/-}$ MEFs only when co-transfected with SIRT1, but not when using the catalytically inactive mutant SIRT1 (H363Y) (Supplementary Fig. 2c). Next, we investigated whether H3K4 methylation levels at circadian promoters are modified by changing NAD$^+$ concentration (Fig. 1e). ChIP experiments on NAD$^+$ and β–NMN-treated cells show that H3K4me3 levels become constitutively low, and that oscillation is partially or totally lost, and these treatments had no effect in *Sirt1*$^{-/-}$ MEFs (Supplementary Fig. 2d). Concomitantly, H3K4me3 and H3K4me2 levels were higher after treatment with FK866, a specific chemical inhibitor of NAMPT[11], showing greater amplitude in oscillation than non-treated cells (Supplementary Fig. 2e). As expected, these changes are accompanied by decreased oscillation of H3 acetylation after FK866 treatment (Supplementary Fig. 2e).

SIRT1 controls MLL1 methyltransferase activity

Based on these findings, we reasoned that SIRT1 could directly modulate MLL1 function[5]. Co-expression of Flag–MLL1–myc and a tagged version of SIRT1 followed by co-immunoprecipitation revealed that SIRT1 interacts with MLL1 (Fig. 2a and Supplementary Fig. 3a). The interaction is specific as shown by the use of the related deacetylase SIRT2

(Fig. 2a). Endogenous SIRT1 and MLL1 proteins also interact as demonstrated by co-immunoprecipitation assays (Fig. 2b and Supplementary Fig. 3b,3c). We next followed the MLL1–SIRT1 interaction along the circadian cycle (Fig. 2c). Nuclear extracts at different circadian times were prepared from DEX-entrained MEFs. Circadian rhythmicity was confirmed by monitoring the oscillation in BMAL1 phosphorylation[25,26] (Fig. 2c). Co-immunoprecipitation assays revealed that MLL1 interacts with endogenous SIRT1 in a circadian time-specific manner. This interaction peaked at CT30–CT36, paralleling *Dbp* circadian profile when H3K4 methylation is at its trough (Fig. 1,2c). The MLL1–SIRT1 interaction was not detected in unsynchronized WT MEFs (Fig. 2c, CT0), indicating that the clock machinery promotes this molecular interplay.

To identify the regions involved in SIRT1–MLL1 interaction, we generated various truncated Flag-tagged versions of the MLL1 protein (Fig. 2d, F–M1 to F–M6). After co–expression in 293 cells, co-immunoprecipitations of SIRT1 with the various MLL1 truncations revealed that an N–terminal region of MLL1 containing its DNA binding domain (aa 650–1327) interacts with SIRT1, confirming specificity of the interaction. (Fig. 2e and Supplementary Fig. 3d,3e). Importantly, this protein domain is involved in the interaction of MLL1 with different protein complexes, regulating its recruitment to specific promoters in the genome [27,28]. We have previously shown that CLOCK interacts with MLL1, that CLOCK's exon 19 is essential for the interaction, and that MLL1 directs CLOCK recruitment to chromatin[5]. Using a mammalian two-hybrid assay (Fig. 2g), we found that the same MLL1 region required for the interaction with SIRT1 mediates the interaction with CLOCK and that MLL1 interaction with CLOCK 19 was much weaker (Fig. 2f).

MLL1 is acetylated

The MLL1–SIRT1 interaction suggested that SIRT1 might control MLL1 through deacetylation, an event that could modulate MLL1 function and activity. To address this question, we first determined whether MLL1 is indeed an acetyl-protein by using ananti pan-acetyl lysine antibody (Fig. 3a and Supplementary Fig. 4a). The interaction between MLL1 and the HATs CBP or p300 has been extensively characterized, including their cooperation in gene activation[29,30]. Thus, we investigated whether CBP or p300 could elicit acetylation of MLL1 (Fig. 3b). Using antipan acetyl–lysine antibody, which preferentially detects C–terminal acetylation of MLL1, we reveal that both CBP and p300 markedly enhance MLL1 acetylation, both at its N– and C– terminal domains. Importantly, PCAF, a HAT related to CBP and p300, does not acetylate MLL1 (Fig. 3b). Specificity was further confirmed since other HATs known to interact with MLL1, including CLOCK[5] and MOF[31], as well as HAT1, do not acetylate MLL1 (Supplementary Fig. 4b).

Next we sought to determine the regulation of MLL1 deacetylation. To do so we co-expressed MLL1 and CBP and then treated cells with HDAC inhibitors Trichostatin A (TSA), which inhibits class I and II HDACs, and-or class III inhibitor nicotinamide (NAM) (Fig. 3c). Acetylation of MLL1 is increased by NAM treatment, but not by TSA treatment (Fig. 3c), indicating that a sirtuin is responsible for MLL1 deacetylation. To establish whether SIRT1 deacetylates MLL1, we used a deacetylation assay (Supplementary Fig. 4c).

Acetyl-MLL1 is readily deacetylated by SIRT1 in a NAD^+ dependent manner (Fig. 3d). This activity is not caused by a possible contamination of the immunoprecipitated proteins with class I or II HDACs since addition of TSA has no effect. Also, previously reported nuclear sirtuins SIRT3, SIRT6 and SIRT7 (Refs. 32-34) are not able to deacetylate MLL1 (Supplementary Fig. 4d), demonstrating that MLL1 deacetylation has to be attributed to SIRT1.

SIRT1-mediated circadian deacetylation of MLL1

While MLL1 acetylation has not been studied previously, mass spectrometry (MS) profiling for global protein acetylome identified four lysine residues as acetylated in MLL1[35]. These are K636, K1130, K1133 and K1235 in the human isoform of MLL1[35]. Interestingly, K1130, K1133 and K1235 are located within the MLL1 region that interacts with CLOCK and SIRT1 (Fig. 2d,2e). Importantly, K1130 and K1133 are highly conserved (Supplementary Fig. 5a), indicating a likely role for acetylation at these two residues. Mutations at K1130 and K1133 into arginine result into a protein that is functionally unable to compete with MLL1-mediated activation of CLOCK–BMAL1 of a circadian gene promoter, whereas the wild type form of the peptide is able to do so (Supplementary Fig. 5b). Thus, theK1130 and K1133 residues are functionally relevant for the activity of the complex (Supplementary Fig. 5b). Similar results were obtained when co-expressing SIRT1. We thereby raised a polyclonal antibody that specifically recognizes MLL1 when acetylated at K1130 and K1133 (Fig. 3e). SIRT1 decreases MLL1 acetylation at K1130 and K1133 (Fig. 3f). In contrast, a catalytically-inactive SIRT1 with a single aminoacid substitution (H363Y), or another sirtuin such as SIRT2, do not influence acetylation at these residues (Fig. 3f). Moreover, pharmacological inhibition of endogenous SIRT1 with EX527 markedly increases K1130 and K1133 acetylation (Fig. 3f), thus confirming that these are specific and direct targets of SIRT1.

As SIRT1 deacetylase activity is circadian[10], we reasoned that its MLL1 target K1130 and K1133 residues could be rhythmically deacetylated. To test this possibility, we entrained cells with dexamethasone and prepared nuclear extracts at various CTs (Fig. 3g). MLL1 shows a robust, circadian acetylation peaking at CT18. Remarkably, MLL1 deacetylation profile parallels its cyclic interaction with SIRT1 (Fig. 2c and Fig. 3g). While the SIRT1–MLL1 interaction peaks at CT30, some deacetylation is observed at CT24. This effect is the results of various factors. First, circadian levels of NAD^+ are high at CT24, enhancing SIRT1 activity and, although at this time its interaction with MLL1 might be weak, deacetylation still occurs stochastically. Second, the specificity of SIRT1 targets is dictated not only by enzymatic kinetics, but also by other components such as additional interacting proteins (i.e. DBC1) or intranuclear availability of NAD^+. Remarkably, the strongest deacetylation of MLL1 is at CT30, coincident with the most efficient interaction with SIRT1. We extended our analysis *in vivo* by preparing liver nuclear extracts at different zeitgeber times (ZT) and then monitored K1130 and K1133 acetylation. MLL1 is acetylated rhythmically in the liver, peaking at ZT9 (Supplementary Fig. 5c). Importantly, genetic ablation of SIRT1 disrupts circadian MLL1 acetylation (Supplementary Fig. 5c), and MLL1 protein levels are not regulated by SIRT1 and remain constant during the circadian cycle (Supplementary Fig. 5d). Remarkably, MLL1 K1130 and K1133 acetylation is enhanced

after FK866 and EX527 treatment as well as in *Sirt1*$^{-/-}$ MEFs, while is lower when cells are treated with NAD$^+$ or β–NMN, demonstrating a molecular crosstalk between MLL1, SIRT1 and energy metabolism (Fig. 3h).

The SIRT1–MLL1 interplay controls circadian transcription

We have previously reported that H3K4me3 at CCGs is mediated by MLL1 (Ref. 5). To investigate whether SIRT1 influences MLL1–mediated function, we analyzed the effect of SIRT1 on the MLL1-mediated activation of the *Dbp* promoter (Supplementary Fig. 6a). As previously reported[5], MLL1 increases CLOCK–BMAL1 dependent *Dbp*-promoter activity in a dose-dependent manner (Supplementary Fig. 6a). This activity depends on the MLL1 catalytic activity, since a mutated protein lacking the catalytic SET domains acts as a dominant negative regulator (Supplementary Fig. 6a). A truncated version of MLL1 lacking a portion of the N–terminal region which includes the two acetylated residues also lost the transactivation potential, highlighting the relevance of this domain in CLOCK–BMAL1 dependent transcription (Supplementary Fig. 6a). Remarkably, SIRT1 strongly reduces CLOCK–BMAL1 mediated transcriptional activation (Supplementary Fig. 6b), an effect dependent on the enzymatic activity since a catalytically inactive SIRT1 (H363Y), is not able to elicit this function (Supplementary Fig. 6b).

To gain insight into the functional implications of the MLL1–SIRT1 interplay, we co-expressed MLL1 with increasing amounts of SIRT1 (Fig. 4a and Supplementary Fig. 6c). Remarkably, SIRT1 decreases MLL1-mediated transcriptional activation of the *Dbp* promoterin a dose-dependent manner (Fig. 4a), an effect abolished when SIRT1 catalytic activity is impaired (Fig. 4a and Supplementary Fig. 6c, SIRT1 (H363Y)). This result was confirmed by pharmacological inhibition of endogenous SIRT1 in cells treated with increasing doses of EX527 (Fig. 4b). Therefore, SIRT1 modulates the MLL1-mediated activation of circadian gene expression. SIRT1-mediated deacetylation has been linked to the function of various transcriptional regulators[36–38]. Thus, we questioned whether MLL1 circadian methyltransferase activity could be controlled by SIRT1. This is indeed the case and SIRT1 deacetylase activity is required for this regulation (Fig. 4c).

Discussion

The cyclic transcription of hundreds clock-controlled genes represents a remarkable paradigm to study harmonic changes in chromatin remodeling [2]. The spatial and temporal organization of the circadian epigenome appears to involve 'nuclear hubs' where coordinately regulated genes are associated in circadian interactomes[39]. The molecular mechanisms that control these events involve chromatin reorganization. Accumulating evidence indicates that a variety of chromatin remodelers are implicated in circadian control, leading to rhythmic acetylation, phosphorylation and methylation of specific residues on histone tails at circadian genes promoters. While a role for CLOCK–BMAL1 in directly influencing chromatin has been proposed[40,41], their recruitment to chromatin loci permissive for transcription most likely involves activator complexes containing enzymatically active remodelers. Among these, MLL1 was shown to play an essential role by directing cyclic

H3K4 tri-methylation and critically contributing to CLOCK–BMAL1 recruitment to chromatin[5].

One unanswered question has been on how chromatin remodelers may interplay to ideally translate changes in cellular metabolism to the homeostatic oscillations in gene expression governed by the circadian clock. In this study we reveal a previously unappreciated connection between NAD^+ and the activity of MLL1, a histone methyltransferase. This link extends to the modulation of H3K4 methylation of CCGs, thereby impacting their transcriptional efficacy (Fig. 5). Our findings support a scenario where oscillating levels of NAD^+ control MLL1 acetylation and thereby CLOCK–BMAL1 dependent transcriptional activation. Specifically, when NAD^+ levels are low, MLL1 is acetylated and cooperates with CLOCK–BMAL1 in circadian gene activation (Fig. 5a). When acetylated, MLL1 enzymatic activity is high (Fig. 4c), paralleling H3K4 trimethylation levels (Fig. 1a,1b) and peak of circadian transcription (Supplementary Fig. 1a,1b). NAD^+ levels rise at ZT11–ZT15, thereby promoting SIRT1 deacetylase activity (Fig. 5b). SIRT1 in turn deacetylates MLL1, an event that reduces its enzymatic activity and leads to decreased H3K4me3 levels (Fig. 5c).

Our findings reveal a yet unexplored regulatory pathway in which clock-driven levels of NAD^+ synthesis lead to cyclic changes in H3K4 methylation, thereby exerting control on clock genes through the interplay of two epigenetic regulators, SIRT1 and MLL1.

It is generally accepted that H3K4me3 plays a major role in transcription-coupled processes[42,43]. Importantly, recent work reveals that manipulation of H3K4me3 levels may impact transcriptional consistency, indicating a role in robustness of transcriptional outputs[44]. Interestingly, stochastic variations in transcription, as well as genome instability[45,46], increase during ageing, and some of these effects are at least partially mediated by SIRT1[47]. Also, it is well established that robustness of circadian gene expression is associated to increased lifespan[14,48,49], and SIRT1 is critical to this mechanism at least in the central pacemaker, the SCN[14]. Here, we provide mechanistic insight into the control of cyclic H3K4me3 levels by SIRT1, indicating that the robust regulation of the circadian epigenome might have potential implications in sustaining correct rhythms on gene transcription.

Finally, the cofactor NAD^+ is emerging as key regulator of metabolism and circadian rhythms[18]. Here we have extended this concept by demonstrating that modulation of intracellular NAD^+ impacts H3K4me3 levels at circadian gene promoters, notably through SIRT1 activation. Importantly, this regulatory pathway does not seem to influence non-circadian MLL1-controlled genes. Thereby, our findings provide an additional paradigm by which metabolism and chromatin remodeling act in concert to keep adequate homeostasis[1,2].

Understanding the mechanisms that enable cells to sense and respond to environmental and metabolic cues trough the circadian clock is of critical importance. The physiological implications of this crosstalk are likely to provide yet unexplored connections between circadian rhythms, cellular homeostasis and aging[50,51]. Our findings reveal a previously unappreciated role of NAD^+–SIRT1 in the control of histone methylation, possibly paving

the way for the exploration of new strategies for therapeutic applications contributing to the modulation of various aging-related diseases.

Online Methods

Animals

4–5 months old male c57BL/6 mice and liver-specific $Sirt1^{-/-}$ mice were housed under 12 hr. light/12 hr. dark (LD) cycles. We used completely randomized experimental designs, in which animals were assigned to each circadian time at random. Sample size was n=5 per time point and genotype for RT-PCR analyses, and n=4 per time point and genotype for protein analyses as previously reported[11–16]. All protocols using animals were approved by the Institutional Animal Care and Use Committee of the University of California, Irvine.

Plasmids

Flag–MLL1–pCXN2, MLL1 carrying the SET domain deletion (Flag–MLL1 SET–pCXN2), Flag–MLL1–myc–pCXN2, myc–CLOCK–pCDNA3, myc–BMAL1–pCDNA3 and *mDbp* and *mPer2* promoters fused to luciferase have been described previously[5]. The plasmid carrying a deletion of exons 3–5 on MLL1 protein (Flag–MLL1 N–pCDNA3) is a kind gift from Dr. P. Ernst. The plasmid Flag–MLL1–myc–pCXN2 was used as template to generate by PCR the MLL1 truncation fragments, which were subcloned in the NotI–XhoI sites of a Flag–pcDNA3 backbone plasmid. The following primers were used to generate the truncated MLL1 fragments (the sequence is detailed in Supplementary Table 1): Flag–M1: M1TAFw and M1Rv; Flag–M2: M2TAFw and M2Rv; Flag–M3: M3TAFw and M3Rv; Flag–M4: M4TAFw and M4Rv; Flag–M5: M5TAFw and M5Rv; Flag–M6: M6TAFw and M6Rv. The plasmids VP16–M1 to M6 were obtained by digestion of the corresponding plasmids Flag–M1 to M6 with NotI and XhoI restriction enzymes, and subsequent cloning on these sites at pVP16AD vector (Clontech). pGAL4BD–CLOCK–pGM4polyII and pGAL4BD–CLOCK 19–pGM4polyII, Flag–SIRT1–pCDNA3 and Flag–SIRT1(H363Y)–pCDNA3 are described in[10]. The formers were used as a template to obtain the plasmids GAL4BD–SIRT1–pGM4polyII and GAL4BD–SIRT1(H363Y)–pGM4polyII. More precisely, the SIRT1 and SIRT1(H363Y) cDNAs were amplified by PCR from the corresponding plasmids using the primers ClaSIRT1Fw and SacSIRT1Rv (Supplementary Table 1). The PCR fragments were digested with ClaI and SacI restriction enzymes and cloned in a similarly digested pG4MpolyII plasmid. The plasmids Flag–SIRT1–7 were kind gifts from Dr. E. Verdin. The vector myc–SIRT2 was kindly provided by Dr. M. Oshimura. The plasmid Flag–PCAF–pCI was purchased from Addgene, and is described elsewhere[52]. The plasmids HA–p300–pCDNA3 and HA–CBP–pCDNA3 are a gift from Dr. S. Sahar. The myc–MOF–pCDNA3 plasmid was obtained by cloning in the BamHI and NotI sites the MOF cDNA obtained by PCR amplification from total mouse cDNA. The myc–HAT1–pCDNA plasmid is described in[53]. All the vectors were examined and verified by restriction analyses and sequencing.

Antibodies and reagents

The antibodies used in this study are the following: anti H3K4me3: Active Motif #39159; anti H3K4me2 and anti H3K4me1: Abcam #ab7766 and #ab8895; anti H3K9/14Ac:

Diagenode #C15410200; anti MLL1 N–terminal: Active Motif #39829 and Bethyl laboratories #A300–087A; anti MLL1 C–terminal: Bethyl laboratories #A300-374A; anti SIRT1: Millipore #09-844; anti BMAL1: Abcam #ab93806; anti p84: GeneTex #GTX70220; anti Actin: Abcam #ab3280; anti Tubulin: Sigma #T5168; anti Acetylated Lysine: Cell Signaling #9441; anti Flag M2: Sigma F7425; anti Myc tag: Millipore #05-419; anti GAL4 (DBD): Santa Cruz #SC-510; anti HA tag: Millipore #05-904. The anti Flag M2 Affinity Gel used for immunoprecipitation of Flag-tagged proteins was purchased from Sigma (#2220). All purchased antibodies are validated for mammalian studies at the manufacturer's website. The rabbit polyclonal anti acetyl-lysines K1130 and K1133 from human MLL1 was generated by immunizing rabbits with KHL-conjugates of the peptide NH2-APPIK(ac)PIK(ac)PVTR (Millipore). Specificity of the antibody was validated by performing the appropriate controls, as depicted across the text, and original images of blots presented in this study can be found in Supplementary Data Set 1. EX526 was purchased from Tocris Bioscience. FK866 was purchased from Axon Medchem. NAD$^+$ (N8535), nicotinamide (N0636), β–Nicotinamide mononucleotide (N3501) and nicotinic acid (N0765) were purchased from SIGMA.

Cell culture

HEK293 cell were maintained in DMEM high glucose (HyClone) supplemented with 10% (v/v) fetal bovine serum (FBS, GIBCO) and antibiotics. MEFs from SIRT1 and MLL1 knockout mice were obtained as described previously [5,10], and cultured in DMEM supplemented with 5% FBS, 5% NBCS (Newborn calf serum, GIBCO) and antibiotics. The stably transfected MEF cell line *Mll1$^{-/-}$/Flag–Mll1* is a kind gift from Dr. J. Hess and is described in [22,27]. All cell lines were tested negative for mycoplasma contamination.

SIRT1 inhibitor "EX527" treatment experiments

MEFs in growing phase (60∼80% confluent) were synchronized with dexamethasone (DEX)[54]. DEX was washed out, and synchronized cells were treated during 18 hours with 50 μM EX527 prior to harvesting for each time point. For CT0, cells were treated with EX527 during 18 hours before and during synchronization. For CT 12, EX527 was added in the media during the 2 hours of DEX synchronization.

Luciferase reporter gene assay

293 cells or MEFs were seeded as a monolayer in 24-well plates. Semiconfluent cells (70–80%) were transfected with 25 ng of luciferase reporter and *LacZ* plasmids, respectively, together with (or without) 50 ng of CLOCK and BMAL1 in the presence or absence of increasing amounts of MLL or SIRT1 plasmids, by using BioT transfection reagent (Bioland) according to the manufacturer's instructions. The total amount of applied DNA per well was adjusted by adding pcDNA3 vector. The amount of each transfected cDNA was determined by considering their molecular sizes and promoter strength of each vector. At 16 hors post transfection, the culture medium was replaced with new one. The luciferase activities were measured 36 hours after transfection as described[55]. The luciferase activities were normalized to transfection efficiency by a colorimetric β–galactosidase assay. For all the transfections presented across the manuscript, control experiments were performed with

or without CLOCK–BMAL1 transfections to ensure that in these conditions on *Dbp*–Luc reporter: 100 ng of CLOCK–BMAL1 transfection leads to $\sim$ 6 times more transactivation than *Dbp*-luc alone, and 300 ng of MLL1 addition is equivalent to $\sim$ 30 times more transactivation.

Treatments on transiently transfected cells

The indicated concentrations of each compound were added to the cells in new culture medium 16 hour post transfection. Cells were harvested for luciferase assays after 16 hours.

Preparation of cell extracts and nuclear extracts

Harvested cells were washed twice with cold phosphate-buffered saline (PBS) and lysed 15 min at 4°C in RIPA buffer supplemented with HDAC inhibitors (50 mMTris-HCL pH 8.0, 150 mMNaCl, 5mM EDTA, 15 mM MgCl$_2$, 1% NP40, 1× protease inhibitor cocktail [Roche], 1mM DTT, 1mM PMSF, 1μM TSA, 10 mM NAM). Lysates were cleared by centrifugation and the supernatants were stored at −80°C. For preparing the nuclear extracts from cells, after the PBS washes, 3×10^7 cells were resuspended and washed twice in fresh hypotonic buffer (10 mM HEPES pH 7.9, 10 mM KCl, 1.5 mM MgCl$_2$, 0.5 mM DTT, 1× protease inhibitor cocktail [Roche]) by collecting them using centrifugation during 10 minutes at 600 g. The pellets were resuspended in 500 μl of Buffer II (hypotonic buffer + 0.1% NP40) and mixed at 4°C during 10 minutes. After a centrifugation step during 10 minutes at 4°C, the supernatant was recovered and stored at −80°C as the cytoplasmic fraction. The pellet containing the nuclear fraction was washed twice with hypotonic buffer and resuspended in 700 μl of hypertonic buffer (20 mM HEPES pH 7.9, 450 mM NaCl, 1.5 mM MgCl$_2$, 1% NP-40, 10% glycerol, 0.5 mM DTT, 1× protease inhibitor cocktail [Roche]) The solution was incubated on ice for 10 minutes, and agitated at 4°C for 30 minutes. After a 10 minutes centrifugation at 4°C and maximum speed, the nuclear fraction was recovered from the supernatant. The nuclear extracts from mice liver tissue was obtained as follows: one quarter of frozen liver was minced and suspended on 5 ml of fresh and ice cold Buffer A (10 mM HEPES pH 7.8, 25 mM KCl, 320mM sucrose, 0.3% triton, 1mM EGTA, 1 mM EDTA, 0.5 mM spermidine, 150 μM spermine, 0.5 mM PMSF, 1mM DTT, 10 mM NaF, 1× protease inhibitor cocktail [Roche]). The liver tissue was then homogenized using a motorized tissue grinder. The samples were washed twice in Buffer A using centrifugations at 3000 rpm during 10 minutes at 4°C each. The pellets were resuspended in 1 ml of ice cold Low Salt Buffer (10 mM HEPES pH 7.8, 25 mM KCl, 20% glycerol, 1mM EGTA, 1 mM EDTA, 0.5 mM spermidine, 150 μM spermine, 0.5 mM PMSF, 1mM DTT, 10 mM NaF, 1× protease inhibitor cocktail [Roche]) and washed twice at 2000 rpm during 10 minutes at 4°C. The pellets were then resuspended in 1 volume of Low Salt Buffer, and 2 volumes of High Salt Buffer (Low Salt Buffer with a final concentration of 0.5 M KCl) were subsequently added. After mixing, the suspension was nutated for 45 minutes at 4°C. The samples were centrifuged for 20 minutes at maximum speed and 4°C, and the supernatants were recovered and stored at -80°C as liver nuclear extracts.

ChIP assays

After dexamethasone synchronization[54], cells were crosslinked at the time points of interest with 1% formaldehyde at room temperature for 15 minutes. The reaction was stopped by adding glycine to a final concentration of 125 mM. The cells were scrapped and suspended on ice-cold PBS. After centrifugation (800 rpm, 10 minutes at 4°C), the cells were washed with 1 ml of ChIP Buffer I (10 mM HEPES pH 6.5, 0.25% triton, 10 mM EDTA, 0.5 mM EGTA) and agitated at 4°C during 10 minutes. The pellets were collected by centrifugation (800 rpm, 10 minutes at 4°C) and similarly washed with 1 ml of ChIP Buffer II (10 mM HEPES pH 6.5, 200 mM NaCl, 10 mM EDTA, 0.5 mM EGTA). The pellet was then resuspended in lysis buffer (50mM Tris-HCL pH 8, 1% SDS, 10 mM EDTA, 1 mM PMSF, $1\times$ protease inhibitor cocktail [Roche]) and stored at –80 °C until all the time points were processed. The samples were then sonicated on ice until the crosslinked chromatin was sheared to an averaged DNA fragment length of 0.2–0.6 Kbp. After centrifugation (10 minutes 12,000 g), soluble crosslinked chromatin was diluted 1:10 in immunoprecipitation (IP) buffer (20 mM Tris-HCl pH 8, 1500 mM NaCl, 1% triton, 2mM EDTA, 1mM PMSF, $1\times$ protease inhibitor cocktail [Roche]). The chromatin preparations were pre-cleared by incubation with 60 µl of protein G PLUS-Agarose solution (Santa Cruz Biotechnology #sc-2002) for 2 hours at 4°C under rotation. The protein G was removed by centrifugation; and the precleared chromatin was immunoprecipitated by incubation with the antibody and 60 µl of protein G PLUS-Agarose solution overnight at 4°C. The immunoprecipitates were washed in buffers TSE I (20 mM Tris-HCl pH 8, 0.1% SDS, 1% triton, 150 mM NaCl, 2 mM EDTA) TSE II (TSE I with a final concentration of 500 mM NaCl), Buffer III (10 mM Tris-HCl pH 8, 1% NP40, 1% deoxycholate, 0.25 M LiCl, 1 mM EDTA), and three times with Tris-EDTA (TE) buffer. To reverse the crosslinking, the washed beads were resuspended in 200 ml of direct elution buffer (10 mM Tris-HCl pH 8, 0.5% SDS, 300 mM NaCl, 5 mM EDTA, 0.05 mg/ml Proteinase K) and incubated overnight at 65 °C. A treatment with RNAse A was performed at 37 °C during 30 minutes and samples were extracted twice with phenol-chlorophorm. The DNA was precipitated with ethanol in the presence of 0.1 mg/ml of glycerol as a carrier. The DNA pellets were resuspended in MQ water and stored at –20 °C.

Quantitative Real Time PCR

cDNA was obtained by retrotranscription of 1 µg of total mRNA using iScript cDNA synthesis kit (Bio-Rad) following the manufacturer's instructions. Real-time RT-PCR was done using the real-time CFX96 detection system (Bio-Rad). The PCR primers are detailed in Supplementary Table 1. For a 20 µl PCR, 50 ng of cDNA template was mixed with the primers to final concentrations of 200 nM and mixed with 10 µl of iQ SYBR Green Supermix (Bio-Rad). The reactions were done in triplicates using the following conditions: 3 min at 95 °C, followed by 40 cycles of 30 s at 95 °C and 40 s at 60 °C.

SIRT1-dependent deacetylation assay on MLL1

Flag–MLL1–myc and SIRT1–7 Flag–tagged plasmids were transfected in HEK 293 cells with BioT reagent (Bioland). Cells were lysed 36 h after transfection with modified RIPA buffer (50 mM Tris-HCL pH 8.0, 150 mM NaCl, 5mM EDTA, 15 mM MgCl$_2$, 1% NP40,

1× protease inhibitor cocktail [Roche], 1mM DTT, 1mM PMSF). Equal amounts of total proteins were immunoprecipitated with anti Flag M2 agarose overnight at 4 °C. Immunoprecipitated material was washed twice with Tris-buffered saline (TBS) and one time with SIRT deacetylation buffer (50 mM HEPES pH 7.5, 50 mM NaCl, 4 mM $MgCl_2$, and 1 mM DTT). The beads with Flag-SIRT1 were distributed in different tubes, according to the number of reactions, and the supernatant was removed. The Flag–MLL1–myc tagged protein was eluted from the agarose beads with Flag peptide (SIGMA #F3290) previously reconstituted in SIRT deacetylation buffer, and equal amounts of this extract were added to the Flag-SIRT1 containing tubes. The reactions were set up in a final volume of 60 μl of SIRT deacetylation buffer supplemented with the adequate compounds (NAM 1 mM, NAD^+ 1 mM or TSA 400 nM). The reactions were incubated during 2.5 hours at 37 °C, stopped by the addition of Laemmli sample buffer, boiled, and after a brief centrifugation, analyzed by western blot.

MLL1 methyltransferase assay

Flag–MLL1–myc plasmid was transfected in 293 cells wither alone or in the presence of GAL4BD–SIRT1 or GAL4BD–SIRT1 (H363Y). After 12 hours transfection, cells were treated either with the small molecule inhibitor of SIRT1, EX527 (final concentration 50 μM) or with the vehicle (ethanol) during 24 hours. Cells were harvested in modified RIPA buffer supplemented with deacetylase inhibitors. The expression of the proteins to similar levels was tested by western blot on total extracts. Similar amounts of extracts were subjected to immunoprecipitation with anti Flag M2 agarose at 4°C overnight. The immunoprecipitated Flag–MLL1–myc was used for the methyltransferase assay following the protocol described in [56], with some modifications. Briefly, reactions were set up in a final volume of 30 μl of KMT buffer (50 mM Tris-HCl pH 8, 5 mM $MgCl_2$, 4 mM DTT) in the presence of 1.2 μl of S-adenosyl-L-[methyl–^{3}H]-methionine (Perkin-Elmer NET155H001MC) and 1μg of recombinant histone H3.3 (New England Biolabs #M2507S). These were incubated at 30 °C for two hours. 10 μl of each reaction were spotted onto Whatman P-81 paper circles (Whatman #3698-325) and processed for liquid scintillation counting as in [56]. The rest of the reaction was stopped with SDS sample buffer and boiled. After a brief centrifugation, 5 μl were loaded in a 5.5% acrylamide gel for WB analysis with anti myc. The rest was loaded on a 15% acrylamide gel, run, stained with Comassie Brilliant Blue, de-stained and photo documented. The gel was then treated for 1 hour with freshly made enhancer solution (1M sodium salicylate, 2% glycerol), dried and directly exposed to a Kodak Biomax MS film (KODAK #822 2648), using an intensifying screen, at −80°C during 2–4 overnights. Methylated H3.3 was visualized upon developing. Original images of gels, autoradiographs and blots can be found in Supplementary Data Set 1.

Statistics and image analyses

Comparisons between samples were performed using two tailed *t*-test, assuming that data follows a normal distribution assessed using graphical methods and KS test. Statistics were performed with Graphpad Prism 6.0 software. Western blot analyses and image processing were performed using ImageJ software.

Supplementary Material

Refer to Web version on PubMed Central for supplementary material.

Acknowledgments

References

1. Feng D, Lazar MA. Clocks, metabolism, and the epigenome. Molecular cell. 2012; 47:158–67. [PubMed: 22841001]

2. Aguilar-Arnal L, Sassone-Corsi P. Chromatin landscape and circadian dynamics: Spatial and temporal organization of clock transcription. Proceedings of the National Academy of Sciences of the United States of America. 2014

3. Koike N, et al. Transcriptional architecture and chromatin landscape of the core circadian clock in mammals. Science. 2012; 338:349–54. [PubMed: 22936566]

4. Ripperger JA, Schibler U. Rhythmic CLOCK–BMAL1 binding to multiple E-box motifs drives circadian Dbp transcription and chromatin transitions. Nature genetics. 2006; 38:369–74. [PubMed: 16474407]

5. Katada S, Sassone-Corsi P. The histone methyltransferase MLL1 permits the oscillation of circadian gene expression. Nature structural & molecular biology. 2010; 17:1414–21.

6. Gut P, Verdin E. The nexus of chromatin regulation and intermediary metabolism. Nature. 2013; 502:489–98. [PubMed: 24153302]

7. Masri S, Sassone-Corsi P. Sirtuins and the circadian clock: bridging chromatin and metabolism. Science signaling. 2014; 7:re6. [PubMed: 25205852]

8. Katada S, Imhof A, Sassone-Corsi P. Connecting threads: epigenetics and metabolism. Cell. 2012; 148:24–8. [PubMed: 22265398]

9. Lu C, Thompson CB. Metabolic regulation of epigenetics. Cell metabolism. 2012; 16:9–17. [PubMed: 22768835]

10. Nakahata Y, et al. The NAD^+-dependent deacetylase SIRT1 modulates CLOCK–mediated chromatin remodeling and circadian control. Cell. 2008; 134:329–40. [PubMed: 18662547]

11. Nakahata Y, Sahar S, Astarita G, Kaluzova M, Sassone-Corsi P. Circadian control of the NAD^+ salvage pathway by CLOCK–SIRT1. Science. 2009; 324:654–7. [PubMed: 19286518]

12. Ramsey KM, et al. Circadian clock feedback cycle through NAMPT-mediated NAD^+ biosynthesis. Science. 2009; 324:651–4. [PubMed: 19299583]

13. Asher G, et al. SIRT1 regulates circadian clock gene expression through PER2 deacetylation. Cell. 2008; 134:317–28. [PubMed: 18662546]

14. Chang HC, Guarente L. SIRT1 mediates central circadian control in the SCN by a mechanism that decays with aging. Cell. 2013; 153:1448–60. [PubMed: 23791176]

15. Masri S, et al. Partitioning Circadian Transcription by SIRT6 Leads to Segregated Control of Cellular Metabolism. Cell. 2014; 158:659–72. [PubMed: 25083875]

16. Bellet MM, et al. Pharmacological modulation of circadian rhythms by synthetic activators of the deacetylase SIRT1. Proceedings of the National Academy of Sciences of the United States of America. 2013; 110:3333–8. [PubMed: 23341587]

17. Gomes AP, et al. Declining NAD(+) induces a pseudohypoxic state disrupting nuclear–mitochondrial communication during aging. Cell. 2013; 155:1624–38. [PubMed: 24360282]

18. Imai S, Guarente L. NAD+ and sirtuins in aging and disease. Trends in cell biology. 2014; 24:464–71. [PubMed: 24786309]

19. Mouchiroud L, et al. The NAD(+)/Sirtuin Pathway Modulates Longevity through Activation of Mitochondrial UPR and FOXO Signaling. Cell. 2013; 154:430–41. [PubMed: 23870130]

20. Berger SL. The complex language of chromatin regulation during transcription. Nature. 2007; 447:407–12. [PubMed: 17522673]

21. Cheng HL, et al. Developmental defects and p53 hyperacetylation in Sir2 homolog (SIRT1)–deficient mice. Proceedings of the National Academy of Sciences of the United States of America. 2003; 100:10794–9. [PubMed: 12960381]

22. Milne TA, et al. MLL targets SET domain methyltransferase activity to Hox gene promoters. Molecular cell. 2002; 10:1107–17. [PubMed: 12453418]

23. Yu BD, Hess JL, Horning SE, Brown GA, Korsmeyer SJ. Altered Hox expression and segmental identity in Mll-mutant mice. Nature. 1995; 378:505–8. [PubMed: 7477409]

24. Wang P, et al. Global analysis of H3K4 methylation defines MLL family member targets and points to a role for MLL1-mediated H3K4 methylation in the regulation of transcriptional initiation by RNA polymerase II. Molecular and cellular biology. 2009; 29:6074–85. [PubMed: 19703992]

25. Lee C, Etchegaray JP, Cagampang FR, Loudon AS, Reppert SM. Posttranslational mechanisms regulate the mammalian circadian clock. Cell. 2001; 107:855–67. [PubMed: 11779462]

26. Tamaru T, et al. CK2alpha phosphorylates BMAL1 to regulate the mammalian clock. Nature structural & molecular biology. 2009; 16:446–8.

27. Milne TA, et al. Multiple interactions recruit MLL1 and MLL1 fusion proteins to the HOXA9 locus in leukemogenesis. Molecular cell. 2010; 38:853–63. [PubMed: 20541448]

28. Xia ZB, Anderson M, Diaz MO, Zeleznik-Le NJ. MLL repression domain interacts with histone deacetylases, the polycomb group proteins HPC2 and BMI–1, and the corepressor C–terminal–binding protein. Proceedings of the National Academy of Sciences of the United States of America. 2003; 100:8342–7. [PubMed: 12829790]

29. Ernst P, Wang J, Huang M, Goodman RH, Korsmeyer SJ. MLL and CREB bind cooperatively to the nuclear coactivator CREB–binding protein. Molecular and cellular biology. 2001; 21:2249–58. [PubMed: 11259575]

30. Goto NK, Zor T, Martinez-Yamout M, Dyson HJ, Wright PE. Cooperativity in transcription factor binding to the coactivator CREB–binding protein (CBP). The mixed lineage leukemia protein (MLL) activation domain binds to an allosteric site on the KIX domain. The Journal of biological chemistry. 2002; 277:43168–74. [PubMed: 12205094]

31. Dou Y, et al. Physical association and coordinate function of the H3 K4 methyltransferase MLL1 and the H4 K16 acetyltransferase MOF. Cell. 2005; 121:873–85. [PubMed: 15960975]

32. Liszt G, Ford E, Kurtev M, Guarente L. Mouse Sir2 homolog SIRT6 is a nuclear ADP–ribosyltransferase. The Journal of biological chemistry. 2005; 280:21313–20. [PubMed: 15795229]

33. Michishita E, Park JY, Burneskis JM, Barrett JC, Horikawa I. Evolutionarily conserved and nonconserved cellular localizations and functions of human SIRT proteins. Molecular biology of the cell. 2005; 16:4623–35. [PubMed: 16079181]

34. Scher MB, Vaquero A, Reinberg D. SirT3 is a nuclear NAD^+-dependent histone deacetylase that translocates to the mitochondria upon cellular stress. Genes & development. 2007; 21:920–8. [PubMed: 17437997]

35. Choudhary C, et al. Lysine acetylation targets protein complexes and co-regulates major cellular functions. Science. 2009; 325:834–40. [PubMed: 19608861]

36. Bouras T, et al. SIRT1 deacetylation and repression of p300 involves lysine residues 1020/1024 within the cell cycle regulatory domain 1. The Journal of biological chemistry. 2005; 280:10264–76. [PubMed: 15632193]

37. Peng L, et al. SIRT1 negatively regulates the activities, functions, and protein levels of hMOF and TIP60. Molecular and cellular biology. 2012; 32:2823–36. [PubMed: 22586264]

38. Vaquero A, et al. SIRT1 regulates the histone methyl–transferase SUV39H1 during heterochromatin formation. Nature. 2007; 450:440–4. [PubMed: 18004385]

39. Aguilar–Arnal L, et al. Cycles in spatial and temporal chromosomal organization driven by the circadian clock. Nature structural & molecular biology. 2013; 20:1206–13.

40. Doi M, Hirayama J, Sassone-Corsi P. Circadian regulator CLOCK is a histone acetyltransferase. Cell. 2006; 125:497–508. [PubMed: 16678094]

41. Menet JS, Pescatore S, Rosbash M. CLOCK–BMAL1 is a pioneer-like transcription factor. Genes & development. 2014; 28:8–13. [PubMed: 24395244]

42. Lauberth SM, et al. H3K4me3 interactions with TAF3 regulate preinitiation complex assembly and selective gene activation. Cell. 2013; 152:1021–36. [PubMed: 23452851]

43. Ruthenburg AJ, Allis CD, Wysocka J. Methylation of lysine 4 on histone H3: intricacy of writing and reading a single epigenetic mark. Molecular cell. 2007; 25:15–30. [PubMed: 17218268]

44. Benayoun BA, et al. H3K4me3 breadth is linked to cell identity and transcriptional consistency. Cell. 2014; 158:673–88. [PubMed: 25083876]

45. Bahar R, et al. Increased cell-to-cell variation in gene expression in ageing mouse heart. Nature. 2006; 441:1011–4. [PubMed: 16791200]

46. Dolle ME, Vijg J. Genome dynamics in aging mice. Genome research. 2002; 12:1732–8. [PubMed: 12421760]

47. Oberdoerffer P, et al. SIRT1 redistribution on chromatin promotes genomic stability but alters gene expression during aging. Cell. 2008; 135:907–18. [PubMed: 19041753]

48. Libert S, Bonkowski MS, Pointer K, Pletcher SD, Guarente L. Deviation of innate circadian period from 24 h reduces longevity in mice. Aging cell. 2012; 11:794–800. [PubMed: 22702406]

49. Wyse CA, Coogan AN. Impact of aging on diurnal expression patterns of CLOCK and BMAL1 in the mouse brain. Brain research. 2010; 1337:21–31. [PubMed: 20382135]

50. Chang HC, Guarente L. SIRT1 and other sirtuins in metabolism. Trends in endocrinology and metabolism: TEM. 2014; 25:138–145. [PubMed: 24388149]

51. Orozco-Solis R, Sassone-Corsi P. Circadian clock: linking epigenetics to aging. Current opinion in genetics & development. 2014; 26C:66–72. [PubMed: 25033025]

52. Yang XJ, Ogryzko VV, Nishikawa J, Howard BH, Nakatani Y. A p300/CBP-associated factor that competes with the adenoviral oncoprotein E1A. Nature. 1996; 382:319–24. [PubMed: 8684459]

53. Nagamori I, Cruickshank VA, Sassone-Corsi P. Regulation of an RNA granule during spermatogenesis: acetylation of MVH in the chromatoid body of germ cells. Journal of cell science. 2011; 124:4346–55. [PubMed: 22223882]

54. Balsalobre A, et al. Resetting of circadian time in peripheral tissues by glucocorticoid signaling. Science. 2000; 289:2344–7. [PubMed: 11009419]

55. Hirayama J, et al. CLOCK-mediated acetylation of BMAL1 controls circadian function. Nature. 2007; 450:1086–90. [PubMed: 18075593]

56. Fingerman IM, Du HN, Briggs SD. In vitro histone methyltransferase assay. CSH protocols. 2008; 2008:pdb prot4939. [PubMed: 21356770]
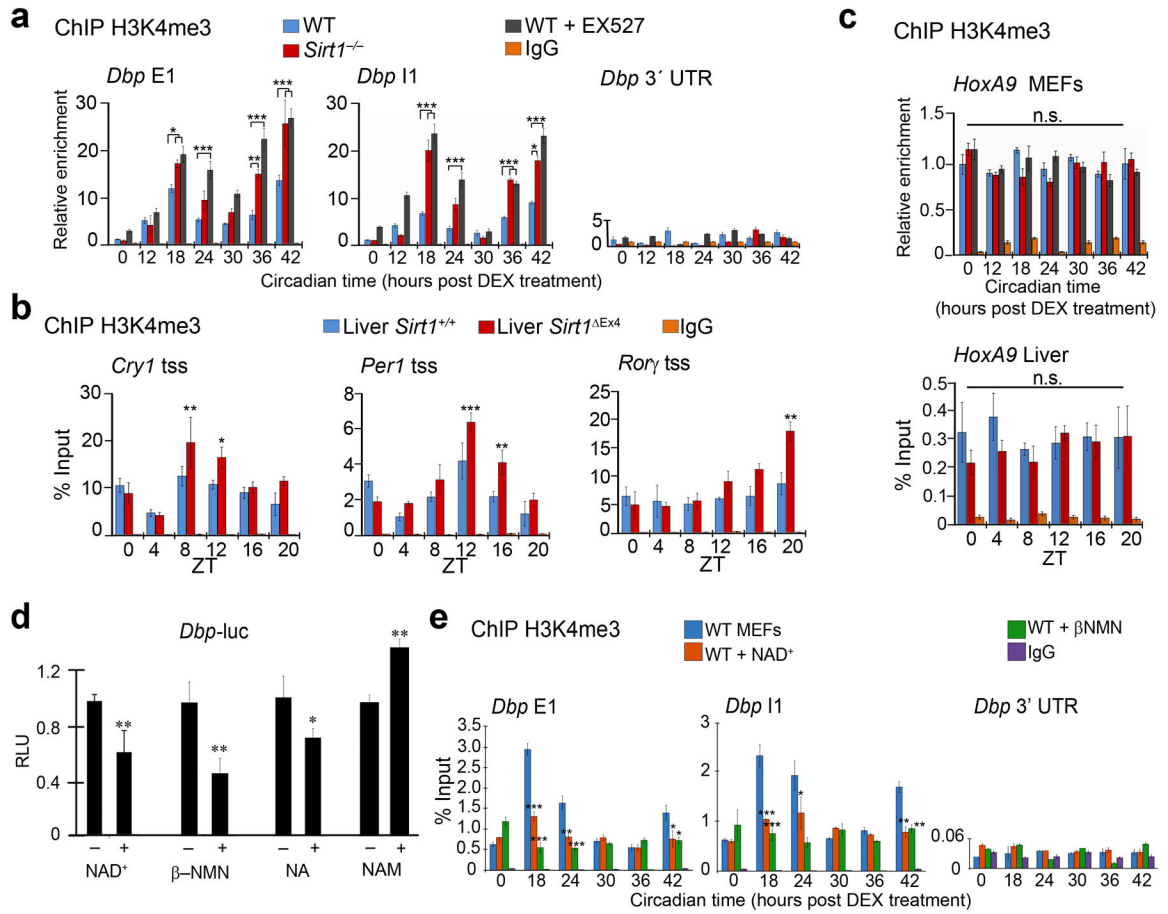
Figure 1. SIRT1 and NAD⁺ levels regulate circadian H3K4 trimethylation

(**a**) ChIP from histone H3K4me3 at specific regions of *Dbp* gene in mouse embryonic fibroblasts (MEFs) from wild type (WT) or *Sirt1⁻/⁻* mice, and WT MEFs treated with EX527 (50μM during 18 hours). Immunoprecipitated chromatin was quantified by real-time PCR, and data from WT samples at time 0 was set to 1. (**b**) H3K4me3 ChIP assays at the transcription start site (tss) of circadian genes in livers from wild type mice and *Sirt1* KO littermates (*Sirt1 ᴱˣ⁴*) harvested at the indicated zeitgeber times (ZT, hours after lights on). (**c**) ChIP from H3K4me3 at *HoxA9* tss either in MEFs (top panel) or in livers (bottom panel). (**d**) Luciferase assay on *Dbp-luc* from 293 cells transfected with MLL1 and CLOCK–BMAL1 plasmids. (β–Nicotinamide adenine dinucleotide: NAD⁺ 2 mM, β–Nicotinamide mononucleotide: β–NMN 5 mM, Nicotinic acid: NA 10 mM, Nicotinamide: NAM 10 mM). Light units were normalized to an internal *LacZ* control, and the relative light units (RLU) from basal expression of *Dbp-luc* from non-treated cells were set to 1 (means ± s.e.m. of four independent experiments). (**e**) ChIP from histone H3K4me3 at indicated regions of the *Dbp* gene from synchronized MEFs either untreated or treated two hours before harvest with 1 mM of NAD⁺or 1 mM of β–NMN. For all ChIP experiments, immunoprecipitated chromatin was quantified by real-time PCR, and means ± s.e.m. of three independent replicates analyzed in triplicates are presented. *P < 0.05, **P < 0.01, ***P < 0.001, two tailed *t*-test.
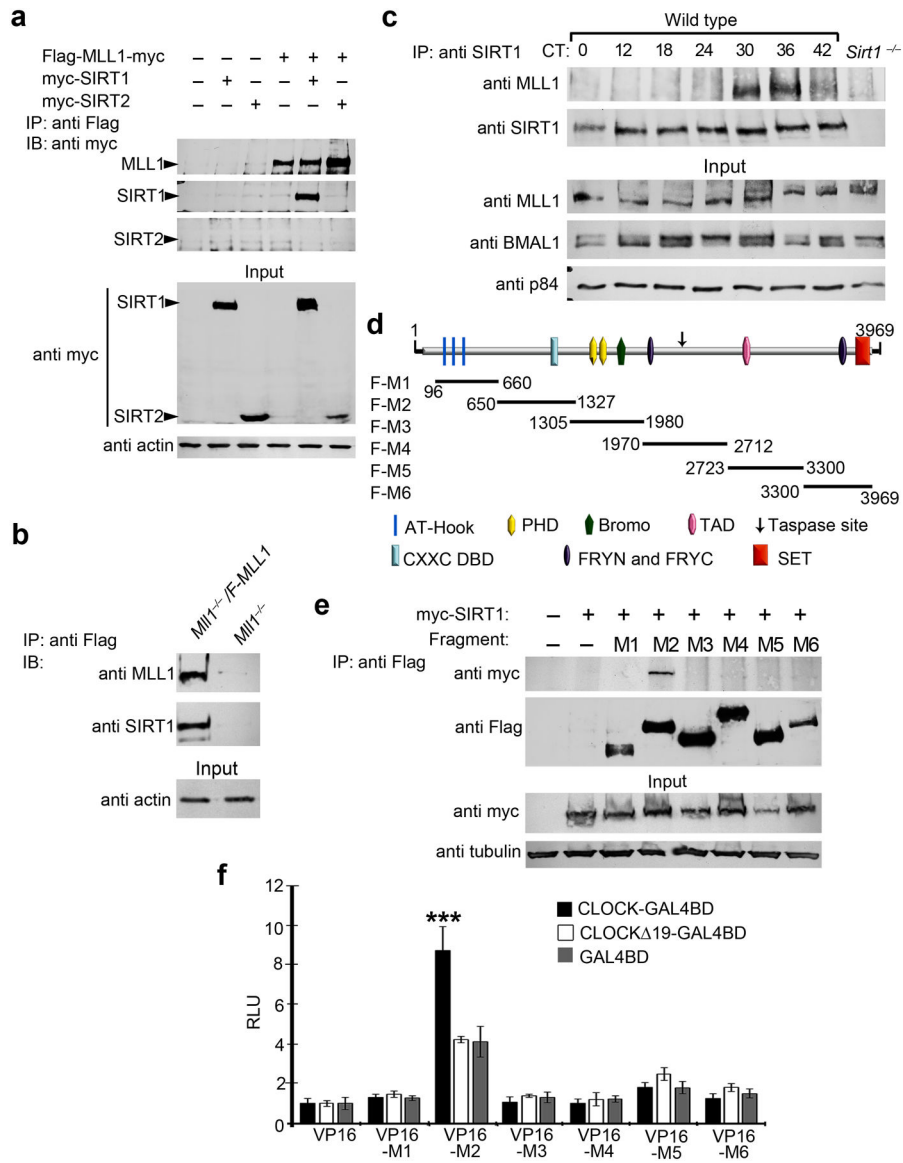
Figure 2. SIRT1 and MLL1 interact
(**a**) Co-immunoprecipitation experiments from 293 cells transiently transfected with the indicated plasmids (IP, immunoprecipitation; IB, immunoblot). (**b**) Co-immunoprecipitation experiments in *Mll1*⁻/⁻ cells and *Mll1*⁻/⁻ stably transfected with Flag–MLL1. (**c**) Co-immunoprecipitation experiments from nuclear extracts of dexamethasone synchronized MEFs with anti SIRT1 antibody. Western blots were performed from immunoprecipitates (top panel) or nuclear extracts (input) at indicated circadian times (CT, hors post DEX synchronization). (**d**) Representation of the localization of the MLL1 truncation domains (M1–M6) used for cloning. (**e**) Co-immunprecipitation experiments using protein extracts from 293 cells transiently expressing the indicated plasmids. (**f**) Mammalian two–hybrid assays in 293 cells transiently transfected with the CLOCK or CLOCK 19 'bait' plasmids (GAL4–CLOCK and GAL4–CLOCK 19) and the respective 'prey' plasmid (VP16 empty control, VP16–M1 to M6). The results are expressed as relative light units (RLU),

representing the activation of the (GAL4–UAS)$_6$–luciferase reporter normalized to the internal *lacZ* control, and units from VP16 empty control were set to 1. Data are presented as the mean±s.e.m. of three independent samples. *$P < 0.05$, **$P < 0.01$, ***$P < 0.001$, two tailed *t*-test.
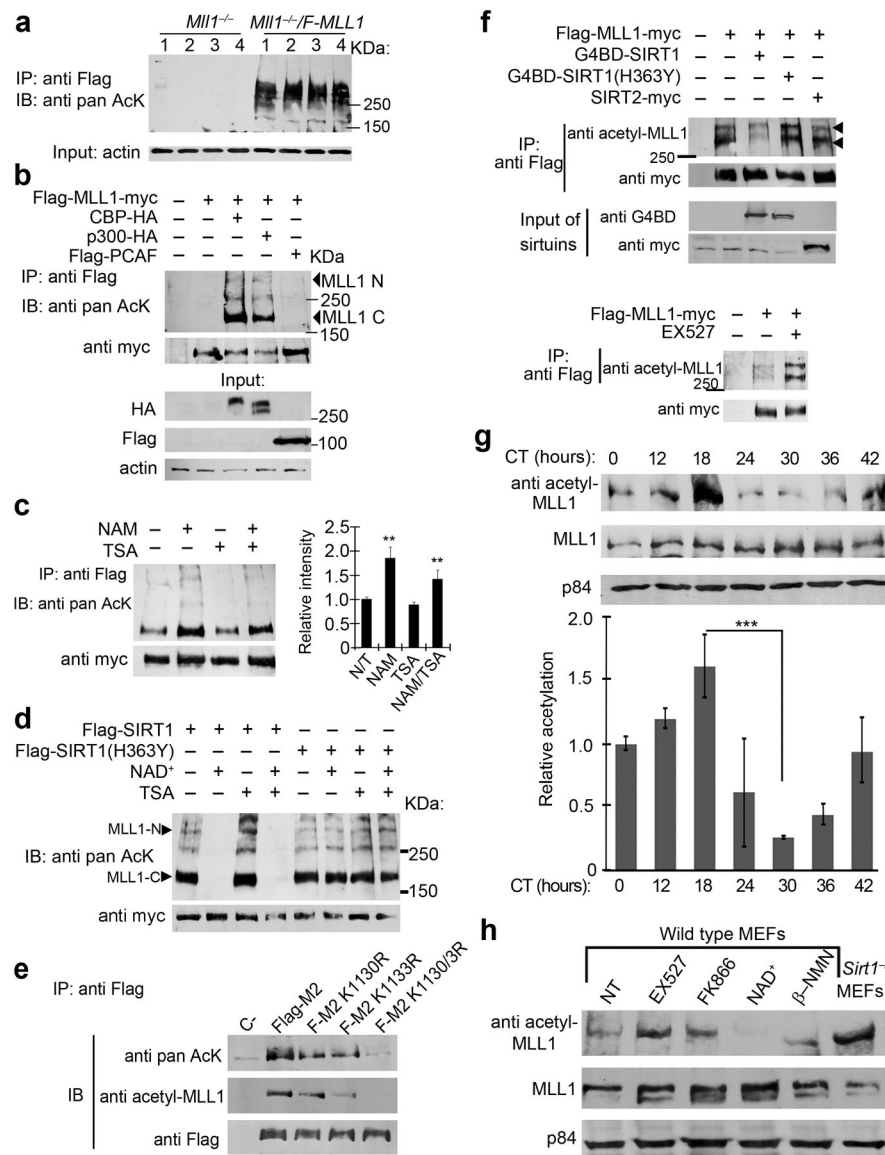
Figure 3. SIRT1 dependent deacetylation of MLL1 controls its activity

(**a**) Immunoprecipitation (IP) with anti Flag followed by western blot (IB) with an anti pan acetyl-lysine (anti AcK) antibody from protein extracts of either *Mll1*⁻/⁻ MEFs or *Mll1*⁻/⁻ stably transfected with Flag–MLL1 (*F–MLL1*). Four independent samples (1–4) are shown for each cell type. (**b**) Immunoprecipitation (IP) and western blot (IB) from total extracts of transiently transfected 293 cells with the indicated plasmids. (**c**) (left) anti Flag immunoprecipitation (IP) from total extracts of 293 cells expressing Flag-MLL1-myc and CBP-HA, and treated with Trichostatin A (TSA, 400 nM) or nicotinamide (NAM, 10 mM) for 16 hr. Western blots (IB) with anti pan acetyl-lysine (AcK) or anti myc for IP, and anti HA, anti Flag and anti actin for input are shown. (Right) histogram represents quantification of acetylated MLL1 normalized to total MLL1. The relative intensity of non-treated samples was set to 1. (Means ± s.e.m. from three experiments; **P < 0.01, two tailed *t*-test). (**d**) MLL1 *in vitro* deacetylation assay using either wild type SIRT1 or a deacetylase-inactive

SIRT1 (SIRT1(H363Y)) with and without NAD^+ and TSA. (**e**) Flag immunoprecipitation from cells expressing the plasmids Flag–M2 wild type or mutated at lysines 1130 (F-M2 K1130R), 1133 (F-M2 K1133R) or both (F-M2 K1130/3R), followed by western blot with the indicated antibodies (anti pan AcK, anti pan acetyl-lysine; anti acetyl MLL1, specific antibody against acetylated lysines K1130 and K1133 from MLL1). (**f**) Anti Flag immunoprecipitation from cells expressing the indicated plasmids followed by western blot using a specific antibody detecting acetylated lysines K1130 and K1133 from MLL1 (anti acetyl-MLL1) or anti myc. At the bottom panels, cells were treated with EX527 (50 μM, 18 hours) (G4BD, Gal4 binding domain). (**g**) Western blot from nuclear extracts of dexamethasone synchronized MEFs at indicated circadian times (CT, hours post DEX synchronization). Histogram shows quantification from acetyl MLL1 normalized to total MLL1. The relative intensity at CT0 was set to 1 (Means ± s.e.m. from three experiments, ***$P < 0.001$, two tailed t-test). (**h**) Western blot for nuclear extracts from MEFs either untreated or treated for two hours with the indicated compounds.
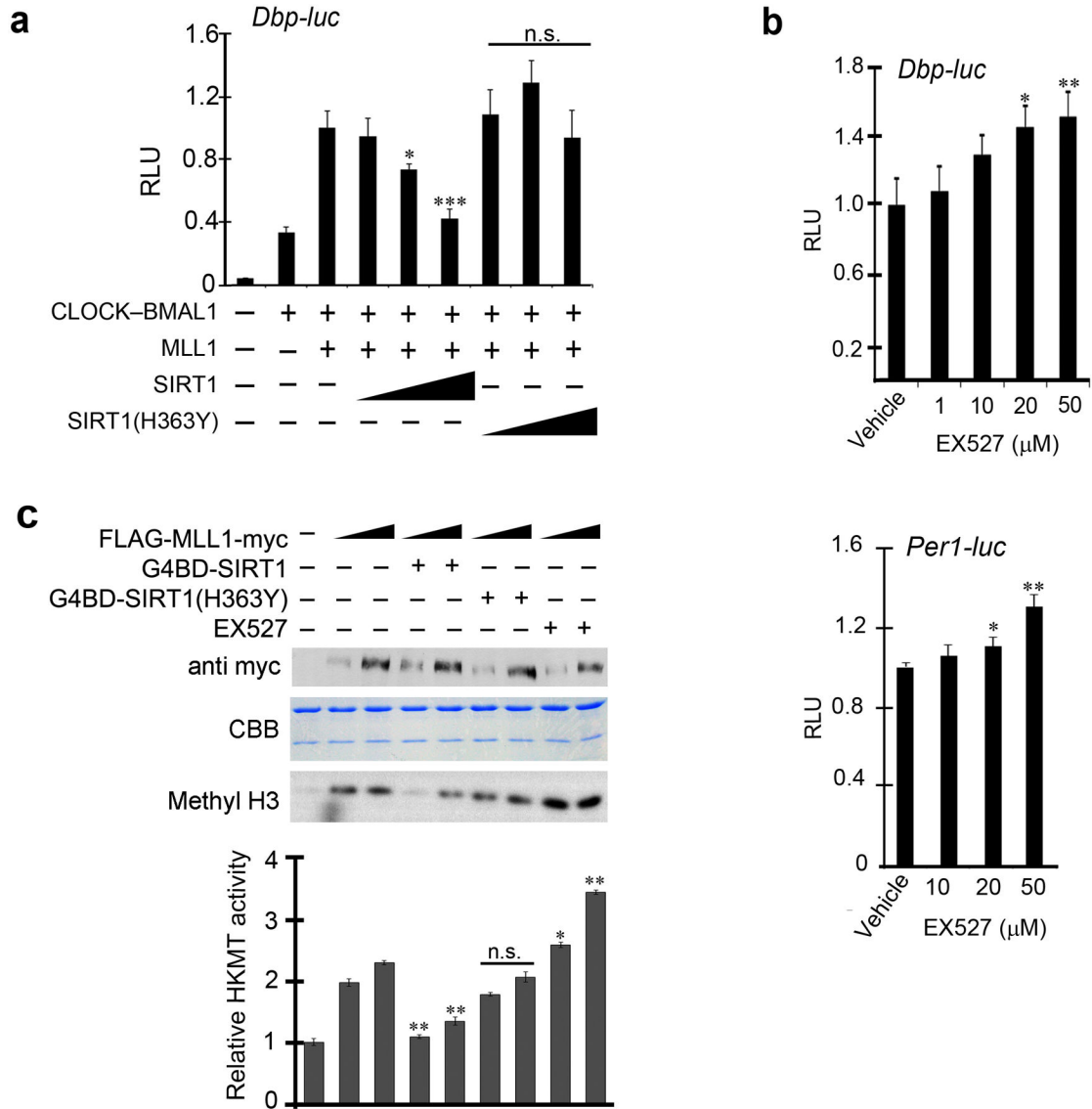
Figure 4. MLL1 H3K4 methyltransferase activity is modulated by SIRT1

(**a**) Luciferase assays using *Dbp*-luciferase reporter in 293 cells transiently transfected with the indicated plasmids. Increasing amounts of plasmids encoding SIRT1 and the mutant form SIRT1(H363Y) were assessed. Light units were normalized to an internal *LacZ* control, and the relative light units (RLU) from basal expression of *Dbp-luc* plasmid were set to 1 (means ± s.e.m. of three independent experiments). (**b**) Luciferase assays using *Dbp*–luciferase (top panel) or *Per1*–luciferase (bottom panel) reporters. Plasmids encoding MLL1 and CLOCK–BMAL1 were transiently transfected in 293 cells. EX527 treatments were performed 18 hours prior to luciferase assays. Light units were normalized to an internal *LacZ* control, and the relative light units (RLU) from basal expression of the reporter from non-treated cells were set to 1 (Means ± s.e.m. of four independent experiments). (**c**) *In vitro* MLL1 histone lysine methyltransferase assay (HKMT) on recombinant histone H3. The top panel corresponds to a western blot from myc-tagged MLL1 protein used for each assay. CBB, Coomassie Brilliant Blue staining from the gel

used to measure radioactive H3. Methyl H3, autoradiography from H3 radioactively labeled with S-adenosyl-L-[methyl-^{3}H]-methionine. Bottom panel, histogram representing quantification of radioactive H3 by liquid scintillation. The counts from the assay without MLL1 protein were set to 1(means ± s.e.m. of three independent measurements). Statistical analyses using two tailed paired t–test are presented; *P < 0.05, **P < 0.01, ***P < 0.001.

Author Manuscript

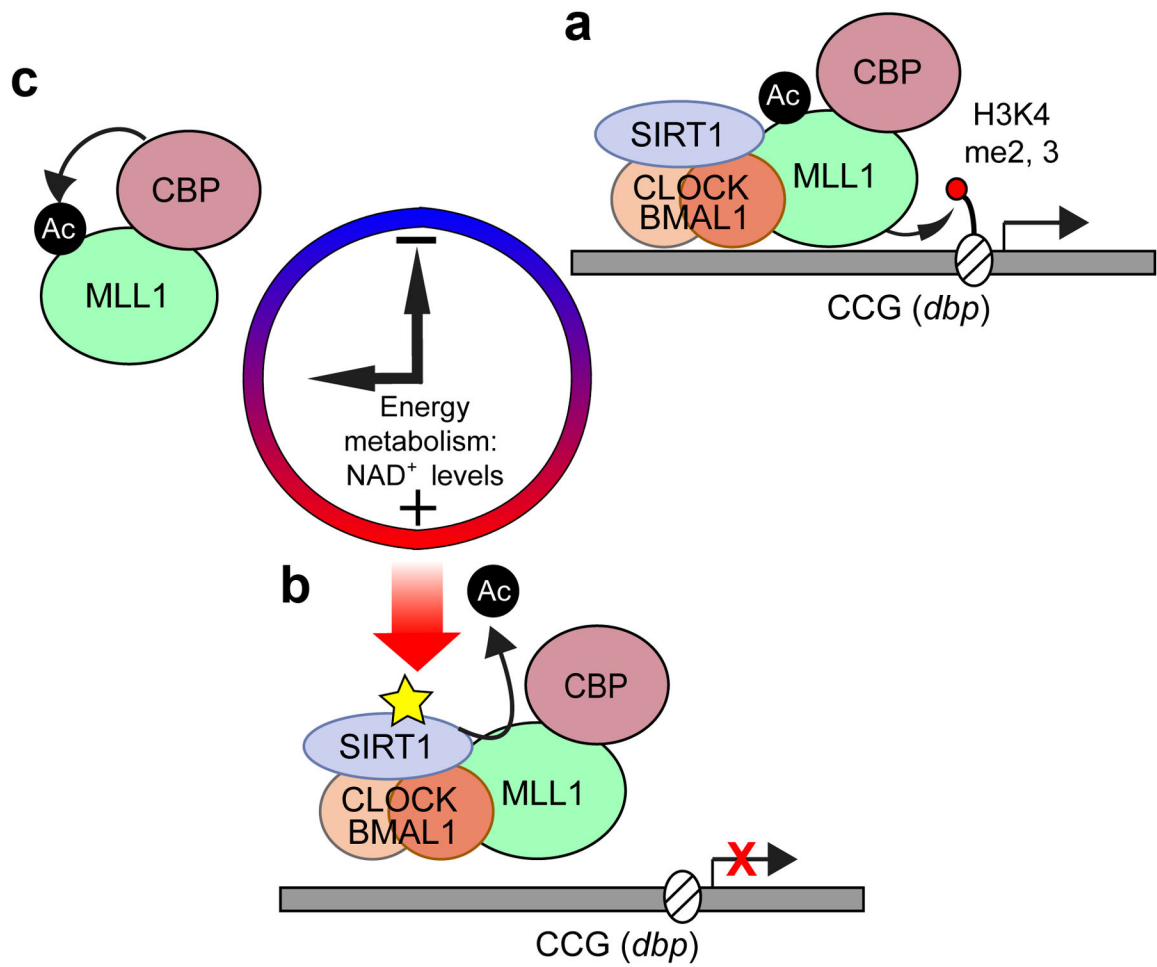Author Manuscript

Author Manuscript

Author Manuscript

Figure 5.
(**a–c**) Model depicting the NAD+–dependent molecular interplay between SIRT1 and MLL1 for the control of circadian gene expression and epigenetic states (see discussion).